

## Stabilization effect in ferroelectric materials during aging in ferroelectric state

Dazhi Sun<sup>a)</sup>

Laboratory for Rare-Earth Functional Materials, Shanghai Normal University, Shanghai 200234, People's Republic of China and National Institute for Materials Science, Tsukuba, 305-0047, Ibaraki, Japan

Xiaobing Ren and Kazuhiro Otsuka

National Institute for Materials Science, Tsukuba, 305-0047 Ibaraki, Japan

(Received 28 March 2005; accepted 31 August 2005; published online 29 September 2005)

We report that aging in ferroelectric state results in an increase of reverse transition temperature  $T_f$  in both BaTiO<sub>3</sub> single crystal and Pb<sub>0.84</sub>La<sub>0.16</sub>Ti<sub>0.96</sub>O<sub>3</sub> polycrystal. This indicates that the ferroelectric phase is gradually stabilized during aging below Curie temperature. The evolution of the stabilization phase with aging time in these two different systems obeys the same kinetic function, but with different relaxation time. This indicates that the stabilization effect of the two systems stems from a common origin. We suggest that the stabilization is due to a short-range ordering of point defects, driven by a symmetry-conforming tendency of point defects. © 2005 American Institute of Physics. [DOI: 10.1063/1.2084343]

Ferroelectric aging is a well-observed fact in all ferroelectric materials. It refers to a gradual change of various physical properties after aging in ferroelectric state.<sup>1,2</sup> As ferroelectric aging strongly affects the properties and stability of the ferroelectric materials, it has received much attention over the past decades, and many models have been proposed to explain the phenomena.<sup>3–9</sup> Some models ascribe the aging effect to certain domain-wall pinning effect, while others ascribe it to grain boundary effect. However, so far there is no unified explanation that can explain all aspects of the ferroelectric aging.

In this letter, we show that there exists a new aspect of the ferroelectric aging so far unrecognized. That is, a gradual increase of reverse transition temperature  $T_f$  (reverse transition finishing temperature) with aging time. We refer to such an aging effect as the “stabilization effect,” as the ferroelectric phase is stabilized during aging. This is an unexpected finding in view of the common sense that Curie temperature is considered as a stable quantity and should not change with time. In the present work, we performed a comparative investigation of the stabilization effect between a simple ferroelectric system, BaTiO<sub>3</sub> single crystals (with low level of oxygen vacancies) and a more complex system Pb<sub>0.84</sub>La<sub>0.16</sub>Ti<sub>0.96</sub>O<sub>3</sub> (PLT) ceramics (which contains more Ti-site vacancies). We found that stabilization occurs in both systems and they show qualitatively the same behavior, but with a difference in speed, which is related to the defect concentrations. Our results suggest that the mechanism of stabilization is the diffusion of point defects inside crystal lattices, driven by a symmetry-conforming short-range-order (SC-SRO) tendency of these defects.

First, we explored the stabilization effect in a BaTiO<sub>3</sub> single crystal, which contains no grain boundary. This experiment can exclude the possible effect of grain boundary. The sample was prepared by a top-seeded solution growth technique. It naturally contains a small amount of Fe<sup>3+</sup> im-

purities and oxygen vacancies (through charge compensation). The sample was cooled through its transition temperature (130 °C) and followed by aging at 60, 80, and 100 °C, for different periods of time. Second, we also studied the stabilization effect of a PLT sample (its Curie temperature is 191 °C.), which was prepared by a conventional solid-route process. The sample was aged at 160, 170, and 180 °C, respectively, for 24–192 h. After aging, the reverse transition finishing temperature  $T_f$  (defined in the inset of Fig. 1) was instantly determined by the differential scanning calorimetry (DSC) measurement (Rigaku Thermo Plus DSC 8230). Here we use  $T_f$  (reverse transition finishing temperature) rather than the peak temperature to characterize the reverse transition temperature, because we want to make a comparison with the similar aging effect in a ferroelastic system.<sup>10</sup> The physical meaning of  $T_f$  is the temperature above which spontaneous polarization disappears completely.

Contrary to the common sense that phase transition temperature should be a fixed temperature for a given ferroelec-

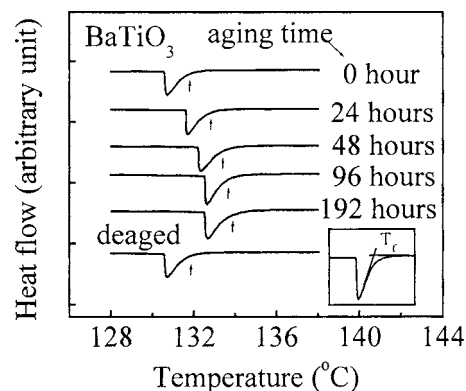


FIG. 1. Shift of DSC peaks of ferroelectric-paraelectric transition of a BaTiO<sub>3</sub> single crystal sample with increase of aging time in ferroelectric state. Aging temperature is 80 °C. Arrows denote the reverse transition finishing temperature,  $T_f$ , as defined by the inset. “Deaged” means that the aged sample is heated to paraelectric phase and held for a certain period to remove the aging effect before cooling again into ferroelectric phase.

<sup>a)</sup> Author to whom correspondence should be addressed; electronic mail: sundazhi@shnu.edu.cn

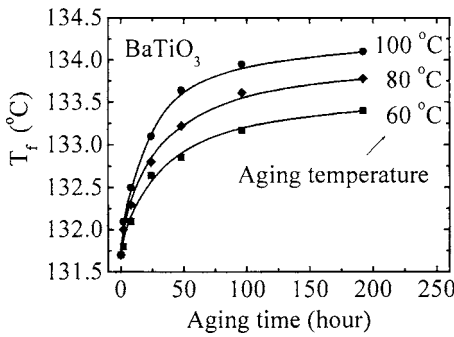


FIG. 2. Reverse transition temperature  $T_f$  of a BaTiO<sub>3</sub> single crystal sample as a function of ferroelectric aging time at different temperatures.

tric crystal, Fig. 1 clearly shows that  $T_f$  of BaTiO<sub>3</sub> single crystal increases with aging time, that is, the stabilization effect exists in a ferroelectric system. Figure 2 shows the relationship between  $T_f$  and aging time and temperature; it is clear that the stabilization effect is stronger when aging temperature is higher. These phenomena demonstrate that the stabilization effect is related to a certain diffusion process, because both longer time and higher temperature are favorable for diffusion.

In order to clarify the stabilization effect, we observed the same effect in another ferroelectric system of the same structure (but with higher vacancy concentration), Pb<sub>0.84</sub>La<sub>0.16</sub>Ti<sub>0.96</sub>O<sub>3</sub> ceramics. As shown in Figs. 3 and 4, stabilization effects are quite similar in these two different systems. Furthermore, we fitted the raise of  $T_f$  with aging time in BaTiO<sub>3</sub> single crystal and Pb<sub>0.84</sub>La<sub>0.16</sub>Ti<sub>0.96</sub>O<sub>3</sub> ceramics, and found that both of them fit well to a Chapman function,  $T_f(t) - T_f(0) = A(1 - \exp(-t/\tau))^{1/2}$ , where  $A$  is the magnitude of the aging effect,  $t$  is aging time, and the relaxation time  $\tau$  is a measure of the aging rate (a detailed account will be presented in another article). From the common kinetics of aging in the two different systems, it seems that the origin of stabilization effect must be related to certain common factors in the two systems. As the size of ferroelectric domains is quite different in these two materials, it is difficult to rationalize the effect in terms of any domain-wall-related process. Furthermore, as BaTiO<sub>3</sub> single crystal does not have grain boundary, any explanation in terms of grain boundary effect can also be excluded. Therefore, the most plausible

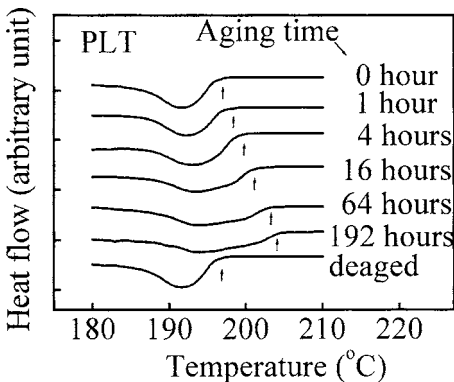


FIG. 3. Shift of DSC peaks of ferroelectric-paraelectric transition of Pb<sub>0.84</sub>La<sub>0.16</sub>Ti<sub>0.96</sub>O<sub>3</sub> ceramics with increase of aging time in ferroelectric state. Aging temperature is 180 °C. (See Fig. 1 for explanation of deaged and arrows.)

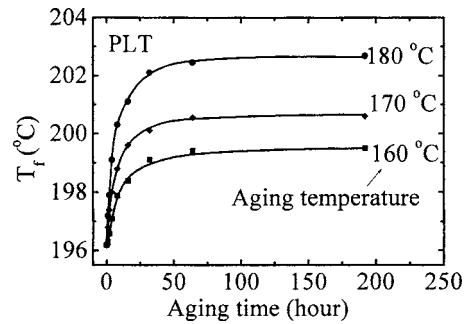


FIG. 4. Reverse transition temperature  $T_f$  of Pb<sub>0.84</sub>La<sub>0.16</sub>Ti<sub>0.96</sub>O<sub>3</sub> ceramics as a function of ferroelectric aging time at different temperatures.

explanation for the stabilization effect seems to be the diffusion of point defects inside crystal lattices.

In the following, we show that the diffusion of point defects inside crystal lattices stems from a simple and common property of defect-containing crystals. We consider a typical ferroelectric crystal with ABO<sub>3</sub> perovskite structure, which contains point defects (such as dopants and vacancies). The idea is also applicable to any other ferroelectric crystals because only symmetry is of relevance. Figure 5 shows the statistical local environment around a given defect (e.g., a heterovalent impurity D<sup>3+</sup> with respect to Ti<sup>4+</sup> in barium titanate) at central site 0 in a perovskite ABO<sub>3</sub> structure. Six oxygen sites form an octahedron. Above the Curie temperature, the crystal symmetry of the paraelectric phase is cubic and centro-symmetrical [Fig. 5(a)]; thus for defect ion D<sup>3+</sup> at central site 0, the six sites at apexes of oxygen octahedron are equivalent, and all cube-corner sites are also equivalent. For such a high-symmetry structure, it is natural that the probability of finding a defect at site  $i$  ( $i=1-6$ ) about the ion D<sup>3+</sup> at site 0 (conditional probability) is equal to that at any other apex of the octahedron, i.e.,  $P_1^d = P_2^d = P_3^d = P_4^d = P_5^d = P_6^d$ , ( $P_i^d \equiv P_i^d | 0^D$ ), where superscript  $d$  denotes defect. This identical probability of defect distribution among equivalent sites corresponds to a cubic symmetry of defect

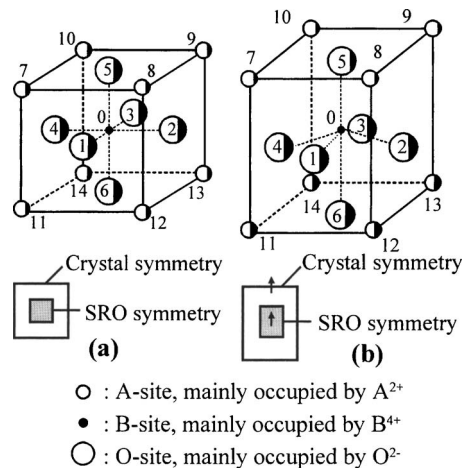


FIG. 5. Symmetry-conforming property of the short-range order (SRO) of point defects in ABO<sub>3</sub> perovskite crystals. Black areas in  $\bullet$  represent the conditional probability of finding a point defect around a given impurity D<sup>3+</sup> in site 0. The crystal symmetry and SRO symmetry can be expressed in a simple symbolic representation as shown below. Square and rectangle represent higher and lower symmetry, respectively. (a) Cubic phase:  $P_2^d = P_3^d = P_4^d = P_5^d = P_6^d$ ,  $P_7^d = P_8^d = P_9^d = P_{10}^d = P_{11}^d = P_{12}^d = P_{13}^d = P_{14}^d$ , (b) tetragonal polar phase:  $P_1^d = P_2^d = P_3^d = P_4^d \neq P_5^d \neq P_6^d$ ,  $P_7^d = P_8^d = P_9^d = P_{10}^d \neq P_{11}^d = P_{12}^d = P_{13}^d = P_{14}^d$ . Arrows in rectangle represent the symmetry with polar axis.

short-range distribution. Following the same reasoning, when a defect occupies cube corners, the same cubic defect symmetry can also be found, i.e.,  $P_7^d = P_8^d = P_9^d = P_{10}^d = P_{11}^d = P_{12}^d = P_{13}^d = P_{14}^d$ . In other words, the probability of finding a certain defect about a given ion (or defect) follows the cubic crystal symmetry. On the other hand, below the Curie temperature, the ion  $D^{3+}$  moves away from the central position. As a result, the associated oxygen octahedron is distorted. A low symmetry ferroelectric phase is formed [Fig. 5(b)]. Some apexes of the octahedron become inequivalent about ion  $D^{3+}$  at site 0. The same situation happens for defects at cube corners. In such a case, interactions between ion  $D^{3+}$  and a defect at inequivalent sites are different. Some SRO configuration must be more stable than others. A typical example is: a negatively charged defect tends to occupy a site near a positively charged ion, rather than a site that is far away. As a consequence, the probability of finding a certain defect about ion  $D^{3+}$  becomes less symmetrical in equilibrium, that is,  $P_1^d = P_2^d = P_3^d = P_4^d \neq P_5^d \neq P_6^d$ ,  $P_7^d = P_8^d = P_9^d = P_{10}^d \neq P_{11}^d = P_{12}^d = P_{13}^d = P_{14}^d$ , conforming to the polar tetragonal crystal symmetry. Therefore, Fig. 5 suggests that, when in equilibrium the probability of finding a point defect around a given ion/defect possesses the same symmetry as the crystal symmetry. This symmetry consideration also applies to sites farther from  $D^{3+}$ , but the effect becomes weaker. Therefore, the effect is a short-range-order (SRO) effect. This is the symmetry-conforming SRO (SC-SRO) property of point defects.

With the symmetry-conforming SRO property of point defects, now it is easy to understand why  $T_f$  of ferroelectric materials increases during aging in the ferroelectric state. When phase transition (from paraelectric to ferroelectric) occurs, crystal symmetry can change abruptly, but point defects stay at their original sites because of the diffusionless nature of such a transition. Therefore, defect symmetry does not match the crystal symmetry, and thus this configuration is unstable. During aging, point defects rearrange (through diffusion) themselves to create a defect symmetry following the crystal symmetry. Then, two symmetries conform to each other and a stable state is formed. From a thermodynamic viewpoint, such a stable ferroelectric state corresponds to a higher  $T_f$  than the un-aged one (i.e., the sample without ag-

ing). This is why  $T_f$  increases with aging time in the ferroelectric state.

Very interestingly, stabilization effect exists in another kind of ferroic materials, martensite/ferroelastic materials.<sup>11</sup> The SC-SRO principle of point defects can explain it as well,<sup>10</sup> even though Coulomb interaction is weak in such systems. Furthermore, another important aging effect, rubber-like behavior in ferroelastic system, is understood by the mentioned mechanism.<sup>12,13</sup> This mechanism has led to a parallel aging effect in ferroelectric systems, the constriction of electric hysteresis loop accompanied with large strain in aged  $BaTiO_3$  single crystals and polycrystals, as revealed by recent study.<sup>14-16</sup> Therefore, the stabilization effect in ferroelectrics reported here indicates that the SC-SRO principle of point defects plays a central role in the aging effect in both ferroelectric and ferroelastic systems. Besides the stabilization effect and constriction of electric hysteresis loop, ferroelectric systems exhibit many other kinds aging behavior; the SC-SRO principle may provide new insight into various aspects of aging effect in ferroelectrics.

The authors thank H. S. Luo for providing single crystal samples. This work was supported by Sakigake-21 of JST and Kakenhi of JSPS. D.S. acknowledges the support from NSF of China (50172055), and Shanghai Shugang Plan (04SG48). D.S. was a recipient of JSPS Fellowship (P02408).

<sup>1</sup>W. A. Schulze and K. Ogino, *Ferroelectrics* **87**, 361 (1988).

<sup>2</sup>K. Uchino, *Ferroelectric Device* (Dekker, New York, 2000).

<sup>3</sup>B. H. Marks, *Electronics* **21**, 116 (1948).

<sup>4</sup>G. Shirane and K. Sato, *J. Phys. Soc. Jpn.* **6**, 20 (1951).

<sup>5</sup>M. C. McQuarrie and W. R. Buessem, *Am. Ceram. Soc. Bull.* **34**, 402 (1955).

<sup>6</sup>W. P. Mason, *J. Acoust. Soc. Am.* **27**, 27 (1955).

<sup>7</sup>K. W. Plessner, *Proc. Phys. Soc. London, Sect. B* **69**, 1261 (1956).

<sup>8</sup>K. Carl and K. H. Haerdtl, *Ferroelectrics* **17**, 473 (1978).

<sup>9</sup>U. Robels and G. Arlt, *J. Appl. Phys.* **73**, 3454 (1993).

<sup>10</sup>X. Ren and K. Otsuka, *MRS Bull.* **27**, 115 (2002).

<sup>11</sup>Y. Murakami, S. Morito, Y. Nakajima, K. Otsuka, T. Suzuki, and T. Ohba, *Mater. Lett.* **21**, 275 (1994).

<sup>12</sup>X. Ren and K. Otsuka, *Nature (London)* **389**, 579 (1997).

<sup>13</sup>X. Ren and K. Otsuka, *Phys. Rev. Lett.* **85**, 1016 (2000).

<sup>14</sup>X. Ren, *Nat. Mater.* **3**, 91 (2004).

<sup>15</sup>L. X. Zhang, W. Chen, and X. Ren, *Appl. Phys. Lett.* **85**, 5658 (2004).

<sup>16</sup>L. X. Zhang and X. Ren, *Phys. Rev. B* **71**, 174108 (2005).